Journal of Aerosol Science 106 (2017) 132–141

Contents lists available at ScienceDirect

Journal of Aerosol Science

journal homepage: www.elsevier.com/locate/jaerosci

In-situ analysis of the gas- and particle-phase in cigarette smoke by chemical ionization TOF-MS☆

Denis J. Phares[a,*,1], Sonya Collier[a,2], Zhongqing Zheng[b,3], Heejung S. Jung[b]

[a] Department of Aerospace & Mechanical Engineering, University of Southern California, Los Angeles, CA 90089, USA
[b] Department of Mechanical Engineering, University of California, Riverside, CA 92521, USA

A B S T R A C T

Mainstream and sidestream smoke samples from two types of cigarette standards (3R4F and 1R5F) were directly analyzed by a chemical ionization mass spectrometer (CIMS). A Walton smoke machine was used to ensure the cigarette is smoked in an acceptably reproducible manner among experiments. Gas-phase material was analyzed in real time and particles were collected on a Nichrome filament, and desorbed at 500° C for analysis immediately after collection was complete. Nicotine was observed to be the most prevalent compound in both phases, indicative of its well-known partitioning behavior. Gas-phase species present in significant amounts in the sidestream samples include benzene, toluene, isoprene, pyridine, 3-ethenylpyridine, xylene, naphthalene, isoquinoline, myosmine, and nicotyrine. Mainstream gas samples exhibited different signatures, dominated by acetaldehyde, acetone, pyrrole, pyrroline, pyrrolidine, and phenolics. These may be indicative of the higher temperature combustion and filtration during each puff. Concentrations of each gas-phase compound were estimated from a mass calibration using toluene vapor. Spectra obtained for the particle-phase contain a complex mixture of high-molecular weight compounds, as previously observed by off-line methods, but also lower molecular weight semi-volatile compounds smaller than nicotine. This gas/particle partitioning may have implications concerning how some of these compounds are absorbed upon inhalation. These compounds are present in the particle-phase and the gas-phase. The soft ionization technique showed a promising result for rapidly identifying chemical differences among cigarette types, smoke streams, and phase.

1. Introduction

The adverse health effects associated with cigarette smoking, combined with its widespread usage, has motivated a large number of chemical, toxicological, and epidemiological studies of the subject of cigarette smoke over many decades. Although the chemicals that comprise tobacco smoke had already been identified by the 1950s (Johnstone & Plimmer, 1959), research activity on the subject has only increased since then. The largest subset of these studies focuses on understanding the biological effects of specific chemical components. Another subset focuses on understanding the fundamental chemistry associated with the formation and evolution of

☆ This study was partially supported by the EPA under STAR grant 832837, and by the California Air Resources Board under contract 06-330. The authors would like to thank Dr. Michael Kleinman for the Walton Smoking Machine and his advice on cigarette smoke generation.

* Corresponding author.
E-mail address: denis@dragonflyenergy.net (D.J. Phares).
[1] Present address: Department of Physics, University of Nevada, Reno, NV, USA.
[2] Present address: Department of Environment Toxicology, University of California, Davis, CA, USA.
[3] Present address: AVL Test System, Inc., Plymouth, MI, USA.

http://dx.doi.org/10.1016/j.jaerosci.2017.01.002
Received 16 September 2016; Received in revised form 11 January 2017; Accepted 13 January 2017
Available online 18 January 2017
0021-8502/

specific chemical components. Yet another aims to quantify the mass of cigarette smoke components in indoor and outdoor urban environments. At least the latter two subsets define a need for instrumentation that can determine the chemical properties of cigarette smoke in real time.

From a fundamental chemistry standpoint, recent studies have focused on the formation of persistent free radicals during pyrolysis of tobacco components (Khachatryan, Asatryan, McFerrin, Adounkpe, & Dellinger, 2010). Such species are stable in the atmosphere, but have damaging biological effects upon inhalation. On-line analysis techniques are required for tracking these relatively short-lived species. From an environmental measurement standpoint, real-time analysis not only minimizes the risk of sample modification prior to measurement, but it also allows for enhanced temporal resolution. As part of their comprehensive study of the sources of fine organic aerosol in the Los Angeles basin, Rogge, Hildemann, Mazurek, Cass, and Simoneit (1994) published a detailed study of the condensed phase organic material in cigarette smoke in an effort to identify tracers for cigarette smoke in the complex urban atmosphere. It was estimated that 2.7% of fine organic particulate matter emissions in Los Angeles were from cigarette smoke. The authors of that study report that the ratio of iso- and anteisoalkanes to *n*-alkanes is highly specific to tobacco. These compounds are also very stable in the atmosphere as opposed to other prevalent potential tracers such as nicotine.

A number of groups have reported the application of on-line chemical characterization to cigarette smoke particles. Barsanti et al. (2007) applied nuclear magnetic resonance NMR spectroscopy to the in-situ chemical analysis of particulate matter in cigarette smoke. More common methods involve collection and vaporization of the condensed material for analysis by mass spectrometry. These studies are more generally concerned with novel techniques for the identification of organic compounds in aerosols, and thus cigarette smoke is merely viewed as an example of a complex aerosol sample. Morrical, Fergenson, and Prather (1998) applied a two-step laser desorption/ionization process for analyzing individual smoke particles. The reported mass spectra are dominated by ion masses that are consistent with PAH skeletons. Oktem, Tolocka, and Johnston (2004) analyzed aerosol particles in cigarette smoke by photoionization aerosol mass spectrometry, wherein particles are collected on a surface in vacuum and desorbed by an infrared laser pulse. The desorbed material is subsequently ionized by VUV radiation and analyzed by TOF-MS. The authors of that study report ion signal at all masses, but single out nicotine as the dominant species. Hearn and Smith (2006) applied an aerosol CIMS instrument to cigarette smoke. In that study, the aerosol sample was vaporized at 300 °C and recondensed in a cooled tube, which was then reheated to 300 °C for analysis of the resulting vapor. Major peaks in those spectra included benzenediol, nicotinic acid, myosmine, nicotine, and cotinine – all of which are consistent with those identified by Rogge et al. (1994). Eschner et al. (2011) applied single-photon time-of-flight (SPI-TOFMS) and quantified 14 gaseous and semivolatile compounds (NO, acetaldehyde, butadiene, acrolein, propanal, acetone, isoprene, furan, crotonaldehyde, isobutanal, butanal, 2-butanone, benzene, and toluene) in cigarette smoke. More recently, Tang, Zheng, Jung, and Asa-Awuku (2012) reported mass spectra obtained by the Aerodyne high resolution time-of-flight (HR-TOF) aerosol mass spectrometer (AMS). Due to the high-energy electron beam impact ionization, *m/z* 43 fragment ions were the most abundant for both main and side stream aerosols. It was also reported that high-intensity peaks are spaced by 14 Da, consistent with the loss of CH_2^+ and N^+ fragments during ionization. Mantz (2007) gave a brief summary of the use of tunable diode laser technology at Phillip Morris over past 25 years to study constituents in cigarette smoke.

In the present study, we apply proton transfer ionization and time-of-flight mass spectrometry (TOF-MS) to the real-time analysis of cigarette smoke. While a majority of other measurement techniques and studies are limited to either phase (between gas and particle) or focused on either smoke (between mainstream and sidestream), we explore the versatility of this relatively soft ionization technique in rapidly identifying chemical differences among cigarette types, smoke streams (mainstream or sidestream), and phase (gas or particle) with a uniquely designed sampling system.

2. Experimental section

2.1. Cigarette smoke generation

Cigarette smoke aerosol is generated using a Walton smoke machine, which was designed to produce mainstream and sidestream smoke in a highly reproducible manner with respect to puffing volume, duration and frequency. The details of the device are available elsewhere (Chen, Namenyi, Yeh, Mauderly, & Cuddihy, 1990), so only the main points are highlighted here. The testing method conforms to the ISO smoking protocol (ISO regimen: ISO3308) for smoking puff volume, duration, and frequency. Mainstream smoke samples are obtained by drawing air through the cigarettes in 2-s puffs every 60 s. Each puff consists of 35 mL of flow per cigarette. The collected mainstream smoke is diluted by an 84 mL/s flow of clean air, yielding a dilution ratio of 140 for one cigarette. The flow is then passed through a 27 L residence chamber where the mixing time is approximately 2 min. The chemical analyzer samples from the residence chamber at a flow rate 0.8 L/min. Sidestream smoke samples are obtained during an identical puff protocol, but the sample aerosol is collected using a funnel placed roughly 10 cm from the ends of the smoldering cigarettes and aspirating a flow of 13.5 L/min. The sidestream sample flow is diluted by air entrained into the funnel along with the smoke, during which the dilution ratio is estimated to be on the order of 2200, based on cigarette plume calculations. The entrained sample is further diluted by a 120 L/min flow, resulting in total dilution ratio of 22,000. The collected sidestream aerosol sample is also held in the 27 L residence chamber prior to introduction into the CIMS.

Two standard cigarette types developed at the University of Kentucky were analyzed. These include the 3R4F (0.73 mg Nicotine per cigarette, 9.40 mg tar per cigarette), and the 1R5F (0.17 mg Nicotine per cigarette, 1.67 mg tar per cigarette). The cigarettes were placed in an airtight plastic bag and stored in a standard laboratory refrigerator until used for the experiment. Mainstream and sidestream samples were analyzed for both standards. Since the mainstream was an intermittent source (i.e. sample generated only during puffs), three cigarettes were consumed at a time. Sidestream samples included one cigarette at a time.

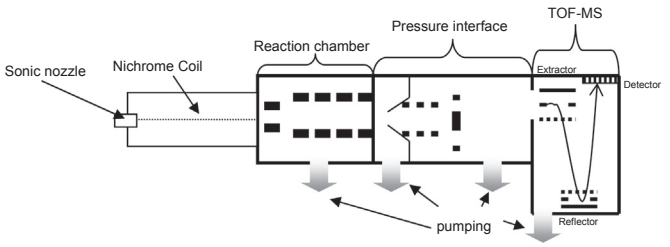

Fig. 1. Schematic of CIMS instrument, including particle collection coil, reaction chamber, pressure interface, and mass spectrometer.

2.2. Chemical ionization mass spectrometer

The CIMS instrument used in this study (shown in Fig. 1) is comprised of a low pressure chemical ionization chamber, a pressure interface, and an orthogonal-extraction reflectron time-of-flight mass spectrometer. The chemical ionization chamber consists of an Americium-241 foil (NRD, Inc) having a radioactivity of 0.5 mCi mounted within a set of electrodes, spaced by static dissipative Teflon. The voltages applied to the electrodes create a constant electric field of 200 V/cm to drive the ions downstream. The chamber pressure is maintained by a single sonic nozzle at 11 Torr, which corresponds to a field strength (E/N) of 53 Td (1 Townsend = 10^{-17} V-cm^2). The sample vapor molecules are ionized by proton transfer from gas phase $(H_2O)_nH_3O^+$ ions, which form from the water vapor that is present in the carrier gas that also transports the sample to the instrument. In this study, filtered compressed air (RH~30%) is used as the carrier gas source. Under these conditions, the total ion production rate was measured by electrometer (Keithley) to be approximately 100 pA.

Ions produced in the reaction region are focused through a 200-micron pinhole into a pressure interface, pumped to 10^{-3} Torr (1 Torr = 133.3 N/m^2) by a Varian V550 turbo pump. The ion transmission efficiency through the pinhole was measured by electrometer to be a few percent. The transmitted ions are then focused into a conical skimmer (Beam Dynamics, Inc.) having a cone tip diameter of 3 mm. The transmission efficiency was found to be highly sensitive to the spacing between the pinhole and the skimmer opening, and the optimum distance was determined to be 21 mm. Beyond the skimmer, the ions are further focused into a tight beam by an Einzel lens. The ion beam is subsequently steered into a chamber, pumped by 2 Varian V70 turbo pumps, and then into the TOF mass spectrometer, which is pumped by a Varian V250 turbo pump. The TOF chamber pressure remained consistently near 10^{-7} Torr.

The TOF chamber (Ionwerks, Inc.) consists of an extractor, a reflector, and an ion detector. The extractor is composed of a back plate, a middle grid, and a grounded front grid. Ions that enter the chamber are steered close to the back plate and are extracted orthogonally from their trajectories when a high voltage pulse is simultaneously applied to the back plate and middle grid. The high voltage pulses are applied at a frequency of 4.5 kHz using fast high voltage transistor switches (Behlke). In general, the pulse frequency is limited by the finite capacitance of the system, which causes excessive current to be drawn from the high voltage power supplies at high pulse frequencies. Ions that are located within the extractor during a high voltage pulse are rapidly accelerated towards the reflector, which spatially refocuses the ions and steers them towards the detector.

The detector consists of two stacked micro-channel plate detectors (Photonis Inc.) in a Chevron configuration, connected to a fast preamplifier and a time-to-digital converter (Ortec). In this way, individual ion impacts are detected and catalogued with respect to the extraction pulse (corresponding to $t = 0$ in the TOF spectrum). Spectra are thus acquired at the extraction pulse frequency of 4.5 kHz. Even at this high frequency, the ion detection rate is only on the order of tens to hundreds per second.

2.3. Performance and calibration

The experimental conditions listed in the preceding section – including pressures, field strengths, and geometrical parameters – represent those that were determined to minimize fragmentation and clustering of the sample ions. As such, the mass spectra obtained for individual organic compounds consist predominantly of the protonated parent ions and have a mass resolution of 150. This resolution does not allow us to deconvolve isobaric ions thus identification of protonated ions presented here are based on the most likely candidates from literature for these tobacco standards. Note that the mass resolution may be increased in future studies by improving the ion focusing optics in the pressure interface as well as the mass spectrometer. These improvements would be necessary for future work sampling more complex mixtures containing unknown compounds. Previous proton transfer mass spectrometry studies (Hanson, Greenberg, Henry, & Kosciuch, 2003; Tanimoto, Aoki, Inomata, Hirokawa, & Sadanaga, 2007) have demonstrated gas-phase sensitivities that are less than ppb for organic standards. Such high sensitivity, however, is not needed for the direct analysis of cigarette smoke. In each of the previous studies, the field strength in the chemical ionization region was several times larger than in the present study. In addition to the enhanced sensitivity, a motivation for keeping the field strength large is to fragment the reactant water cluster ions, so that the gas-phase chemistry remains simple (i.e. only rate constants for reaction with H_3O^+ are needed to quantify sample ionization rates). However, large field strengths also tend to fragment some of the parent ions. Isoprene, for example, begins to fragment at field strengths exceeding 100 Td (Tanimoto et al., 2007).

The field strength applied in the present study (53 Td) resulted in the formation of only $(H_2O)_nH_3O^+$ reactant ion clusters, where the n = 0, 1, 2, and 3 clusters were detected. Other ions that may form in air, including O_2^+ and N_2^+ were not detected, even though air was used as the carrier gas. The resulting spectra are clean, in that primarily protonated parent ions are detected, but the presence

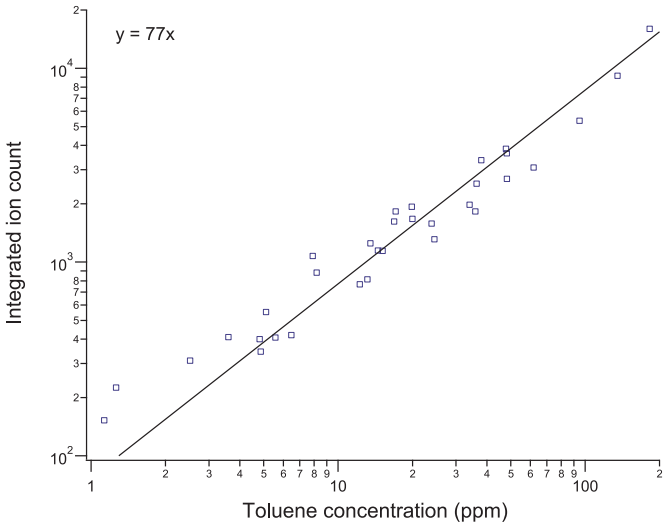

Fig. 2. CIMS sensitivity to controlled concentrations of toluene vapor over a sampling time of 10 min. The solid line represents a linear fit.

of water cluster ions makes mass quantification more difficult. The response of the CIMS-TOF mass spectrometer to known concentrations of toluene was determined in order to estimate the gas-phase concentrations of compounds measured in cigarette smoke. Trace quantities of toluene vapor was introduced by bubbling compressed air through a flask of toluene liquid at 0 °C. The flow rate through the flask was carefully controlled by a calibrated precision needle valve. The resulting ion count within the toluene peak, integrated over 10 min are shown in Fig. 2. The calibration curve is linear for a large range of gas phase toluene concentrations, as indicated by the linear fit in the figure. At higher concentrations, the integrated count is no longer sensitive to the toluene concentration. All gas phase concentrations in the present study were within the linear portion of the curve.

2.4. Particle sampling

Sampling the gas-phase or the particle-phase from cigarette smoke is far from trivial due to the interaction between the two phases that generally results in partitioning of semi-volatile compounds (Chen & Pankow, 2009). Collecting particles on a filter for off-line analysis causes the more volatile components to escape prior to analysis. Similarly, completely removing particles from the flow by filtration for analysis of the gas phase may cause some of the less volatile compounds to adsorb onto the filter and thus be removed from the flow. In the present study, we have made some attempt to maintain the particle/gas interaction by analyzing the gas phase while simultaneously collecting particles onto a Nichrome filament. Thus particles are present in the instrument during gas-phase analysis, but are ultimately either collected by the filament or removed by coarse pumping of the system. The collected particles are then analyzed by thermal desorption immediately after the gas-phase signal dropped below background. Mainstream particles were sampled during the consumption of 9 cigarettes, and sidestream particles were sampled during the consumption of 3 cigarettes.

The particle collector is mounted downstream of the sonic nozzle, and adjacent to the chemical ionization chamber. It is thus maintained at 11 Torr during collection and desorption. Collecting and desorbing the particles at low-pressure facilitates the transport of high-molecular weight vapor into the chemical ionization chamber during desorption of the particles, but may result in some loss of the more volatile species. Nevertheless, this loss was not complete, as these low molecular weight species were indeed detected during the analysis of the condensed phase.

The particle collector consists of a stainless steel cross mounted adjacent to the chemical ionization chamber by a conflat flange. The Nichrome coil filament was stretched 10 cm longitudinally along the direction of flow (as shown schematically in Fig. 1), in order to maximize the deposition of particles along the filament length. Since the Stokes number of the particles is well below unity for even the largest particle sizes, particles that deposit do so primarily by diffusion. The diffusivity, D, of the smoke particles may be calculated by the Stokes-Einstein relation:

$$D = \frac{kTC_c}{3\pi\mu D_p},$$

where D_p is the particle diameter, μ is the gas viscosity, k is the Boltzmann constant, and the temperature, T, was measured to be 11 °C – due to the expansion cooling of the gas as it passes through the sonic nozzle. The Cunningham slip factor, C_c, is an empirical correction to the Stokes drag that accounts for non-continuum effects (i.e. gas slip at the particle surface). It may be written in terms of the gas mean free path, λ (Hinds, 1999):

$$C_c = 1 + \frac{\lambda}{D_p}\left[2.34 + 1.05\exp\left(-0.39\frac{D_p}{\lambda}\right)\right].$$

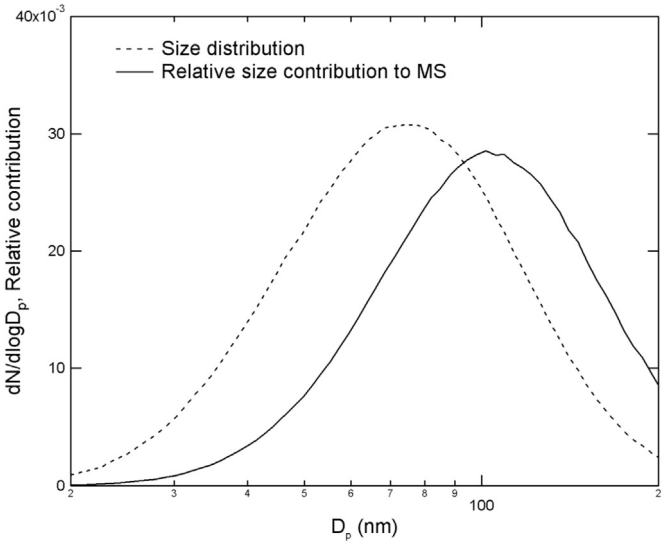

Fig. 3. Size distribution of sidestream aerosol from 3R4F cigarette as measured by SMPS, along with the corresponding contribution to the particle-phase mass spectrum considering diffusion and mass corrections.

Although the deposition fraction may not be precisely computed in this complex geometry, one can estimate an order of magnitude from the root mean square of the displacement, x_{rms}, from the gas streamlines flowing over the filament:

$$x_{rms} = \sqrt{2Dt},$$

where the time, t, is the flow time over the filament. This parameter describes the extent of diffusional spreading of a particle ensemble. As the aerosol flow bends around the filament surface, particles that approach within this distance are likely to deposit on the surface. For a typical smoke particle, 100 nm in diameter, this diffusional spreading is on the order 100 μm, corresponding to a deposition fraction on the order of 0.5% of the particles that initially approach within the filament cross section, which is estimated to comprise 5% of the flow tube cross section, so the net deposition fraction is roughly 0.025%. The total mass deposited per sample is estimated to be on the order tens to hundreds of nanograms.

Although the composition of the particles is not expected to vary with size due to the proximity of the source, one may estimate the size bias in the contribution to the mass spectra of the particle phase. The diffusional deposition efficiency decreases with particle size (and actually scales with the diffusivity, D, raised to the 2/3 power (Hinds, 1999), but the deposited mass per particle increases with the particle size cubed. Taking both of these somewhat offsetting effects into account, the relative contribution to the mass spectra based on the particle size distribution is shown in Fig. 3 for a sidestream sample analyzed by scanning mobility particle size analysis. Although the peak in the size distribution occurs at 75 nm, the most represented particle size in the mass spectrum increases slightly to 100 nm.

3. Results

In general, the obtained mass spectra exhibit chemical characteristics of cigarette smoke that have been previously reported for both gas- and particle-phase samples. Nicotine is the most notable compound in all of the acquired mass spectra. Gas-phase nicotine is in its free-base form, and some fraction of the particulate phase nicotine is protonated (or bound) depending on the pH of the particle. This may have some physiological implications because free-base nicotine is more mobile in tissue than bound nicotine (Pankow, 2001). Unfortunately, it is unlikely that the thermal desorption process could allow for resolution of the bound fraction. When a smoke particle desorbs, the water likely boils off first, leaving behind free-base nicotine, which subsequently volatilizes and then becomes protonated in the gas-phase. The thermal desorption of smoke particles for chemical analysis and the accompanying fate of the dissolved species should be explored in future studies.

3.1. Mass spectra of gas-phase samples

The most notable difference between the mass spectra obtained from 3R4F and 1R5F cigarette standards is the size of the nicotine peak for both sidestream and mainstream samples. For the gas-phase sidestream samples, there is little difference in the mass spectra between the cigarette types (see Fig. 4) other than the size of the nicotine peak. Other prevalent compounds in both sidestream spectra include isoprene, benzene, pyridine, 2-methylfuran, toluene, 3-ethenylpyridine, xylene, indole, naphthalene, isoquinoline, myosmine, and nicotyrine, where identification of the peaks was aided by comparison with previous studies (Eatough et al., 1989; Mitschke, Adam, Streibel, Baker, & Zimmermann, 2005). Using the toluene calibration obtained from Fig. 2, the toluene concentration in the diluted sample is calculated to be 1.7 ppm. It should be noted that, due to their reduced proton affinities,

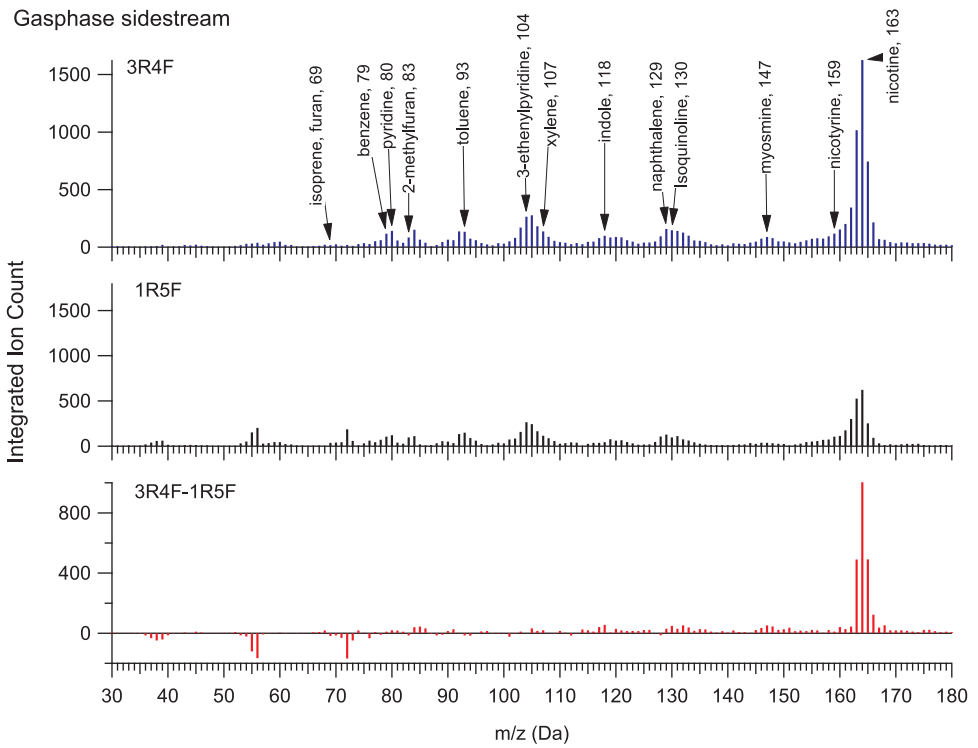

Fig. 4. CIMS-TOF mass spectra of gas-phase sidestream samples from both cigarette types.

small-chain alkanes that are known to be present in gas-phase cigarette smoke in comparably large concentrations (Philippe & Hobbs, 1956), including methane, ethane, propane, and butane, do not react with protonated water (Spanel & Smith, 1998) and are thus not detected in the present study.

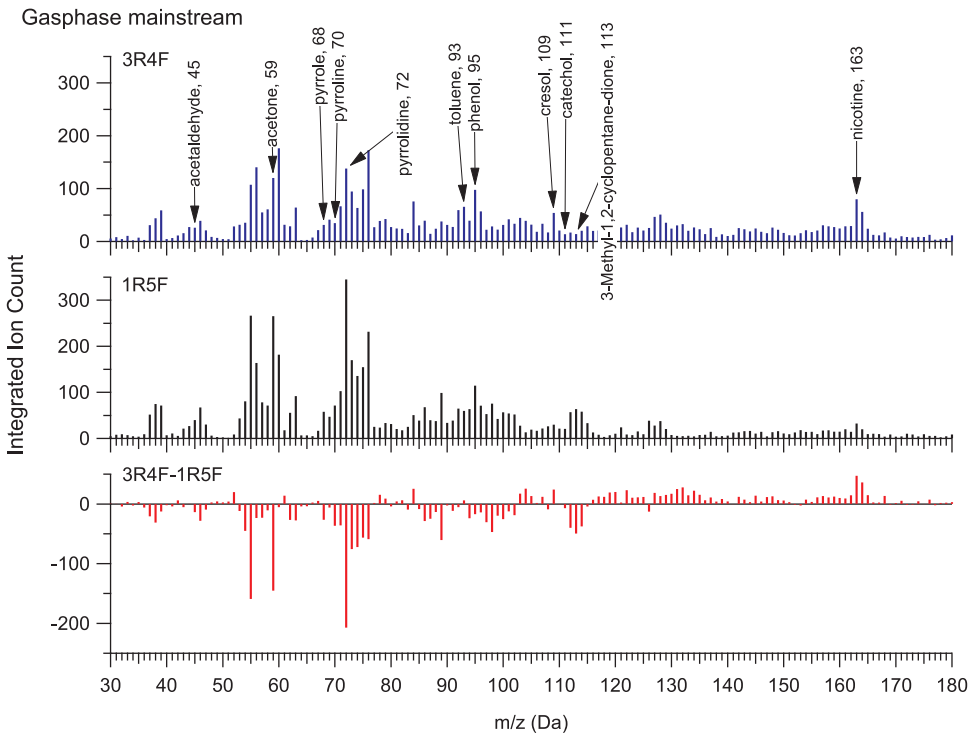

Fig. 5. CIMS-TOF mass spectra of gas-phase mainstream samples from both cigarette types.

The gas-phase mainstream sample spectra, shown in Fig. 5, are dramatically different than the sidestream counterparts. Nicotine is still prevalent in both cigarette types, as are the expected aromatics (benzene, toluene, and pyridine) to a lesser extent. However, the mainstream samples are dominated by other N-ring compounds (pyrrole, pyrroline, and pyrrolidine), phenolics (phenol, cresol, and catechol), acetone, and acetaldehyde, none of which were apparent in the sidestream samples. These compounds may be indicative of the higher-temperature chemistry that exists during a puff. Although some of these compounds do exist in unburned tobacco, they may also have formed through fragmentation of higher molecular weight compounds that might otherwise exist in the particle-phase. This is further evidenced by the detection of a known nicotine fragment, which, when protonated, would exhibit a peak at 85 Da (Hertz, Streibel, Liu, McAdam, & Zimmermann, 2012; Mitschke et al., 2005). This fragment, formed when the pyridine ring splits off of the nicotine molecule, was the most commonly detected ion when VUV ionization was applied to thermally desorbed cigarette smoke particles in the Aerodyne Aerosol Mass Spectrometer (Northway et al., 2007).

From the toluene calibration in Fig. 2, the toluene integrated ion count yields a concentration of 0.85 ppm in the diluted mainstream sample. This diluted concentration corresponds to an average toluene concentration of 31 ppm in the direct mainstream flow of one cigarette, or an average of 5.7 μg of toluene per puff. This value is consistent with previous studies of direct mainstream gas analysis. Brunnemann, Kagan, Cox, and Hoffmann (1990) used gas chromatography to determine that the toluene content in each puff monotonically increases from 1 μg in the first puff to 10 μg in the tenth puff. In an early study, Philippe and Hobbs (1956) used infrared absorption to determine mainstream toluene concentrations to be between 10 and 50 ppm for 2 cigarette types.

Determining the concentrations of the other gas-phase compounds requires knowledge of the mass-dependent ion transmission efficiency from the chemical ionization chamber through the pressure interface and to the detector of the mass spectrometer, as well as the proton transfer reaction rate constant with each protonated water cluster. As long as a sample molecule has a higher proton affinity than water, proton transfer occurs with near unity efficiency upon collision. Therefore, the reaction rate becomes entirely dependent upon the collision rate in the reaction chamber, which is sensitive to the polarizability of the sample molecules. For this computation, we assume that the transmission efficiency is constant for the range of ions detected in the gas-phase, and that the relative reaction rate constant with respect to toluene may be entirely described by reaction with the hydronium ion, H_3O^+, for which some values were tabulated by Zhao and Zhang (2004). The results for a variety of compounds detected in the mainstream flow from the 3R4F cigarette are shown in Table 1. Only compounds for which the rate constant, k, was available are listed in the table; and one compound, 1,3-butadiene, was omitted because of its coincidence with $(H_2O)_2H_3O^+$ at m/z 55.

In general, the tabulated values in Table 1 are in good agreement with previous results (Philippe & Hobbs, 1956) (Brunnemann et al. 1990), though some components are known to exhibit a large variability range among cigarette types (e.g., phenol concentrations may vary by a factor of 10 among cigarette brands (Spears, 1963)). The benzene puff concentration of 27 ppm is in excellent agreement with that reported by Mitschke et al. (2005), who determined a peak benzene concentration of about 30 ppm during the third puff of the similar 2R4F (0.9 mg Nicotine per cigarette, 9.7 mg tar per cigarette) cigarette. Pieraccini et al. (2008) report emission rates from an MS (Italian brand) cigarette of 3.06, 4.64, and 1.09 μg/puff for benzene, toluene, and xylene, respectively. These values are also in relatively good agreement with the corresponding values of 3.36, 5.70. and 1.60 μg/puff from Table 1. The exceptions are isoprene and acetalaldehyde, which are an order of magnitude lower than expected. Isoprene emission rates range from 200 to 400 μg per cigarette (Report on Carcinogens, 2011), which corresponds to tens of micrograms per puff (Brunnemann et al., 1990). Although no quantitative isoprene emission rates have been explicitly reported for the 3R4F or 1R5F cigarette standards, Hertz et al. (2012) recently applied microprobe extraction and photoionization TOF-MS and demonstrated dominant isoprene and acetaldehyde signals during puffs from the 2R4F. Eschner et al. (2011) also reported 317 and 493 μg/puff for isoprene and acetalaldehyde, respectively, from the 2R4F.

3.2. Mass spectra of particle-phase samples

The mass spectra of the particle-phase for both cigarette standards and both sample streams are shown in Fig. 6. The spectra are displayed as an integrated ion count, which ideally scales with the gas-phase concentration within the chemical ionization chamber,

Table 1
Computed mass emissions of selected gas-phase compounds detected in mainstream smoke from the 3R4F cigarette. Values are estimated from the integrated ion count using the toluene calibration, and then corrected using the proton transfer reaction rate constant, k, reported by Zhao and Zhang (2004). Only compounds for which a reaction rate constant is available are listed.

Compound	k (Zhao & Zhang, 2004) (10^{-6} cm^3/s)	Puff Concentration (ppm)	Emission rate (μg/puff)
Isoprene	1.94	27.2	2.89
Benzene	1.97	27.5	3.36
Toluene	2.12	39.6	5.70
Xylene[a]	2.3	9.6	1.60
Naphthalene	2.59	17.5	3.50
Acetone	3.00	51.2	4.64
Acetaldehyde	3.36	9.9	0.68
Furan	1.78	29.7	3.16
Phenol	2.52	49.5	7.28
Cresol[a]	2.5	27.6	4.67

[a] Value averaged over isomers.

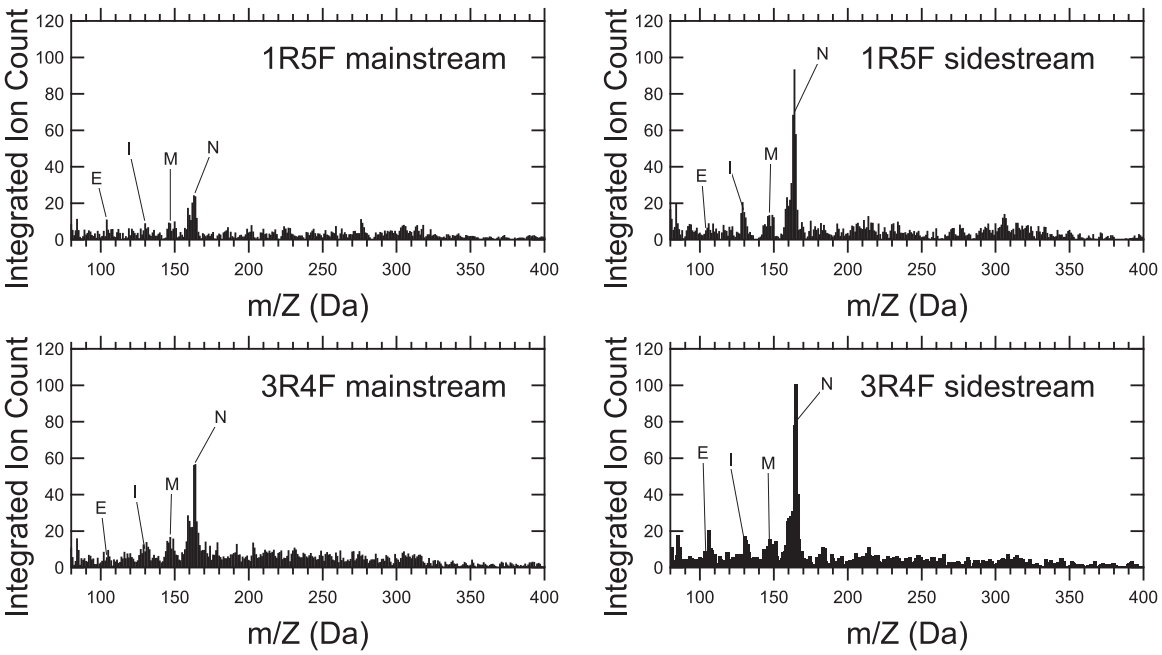

Fig. 6. CIMS-TOF spectra of thermally desorbed particles from mainstream and sidestream smoke for both cigarette types. The labeled prominent peaks are 3-ethenylpyridine (E), isoquinoline (I), myosmine (M), and nicotine (N).

rather than the mass of each compound in the particles. Once again, the most common ion is nicotine and, as expected, the condensed phase contains an almost continuous range of ion masses heavier than nicotine. Also prevalent in all of the particle-phase spectra are nicotyrine, myosmine, isoquinoline, naphthalene, indole, and 3-ethenylpyridine, thereby demonstrating the gas/particle partitioning potential of these lower molecular weight compounds. A notable feature of Fig. 6 is the difference in nicotine content between the low and ultralow cigarettes, which is only apparent in the mainstream samples. Sidestream particle-phase nicotine content is comparable between cigarette types. This is in direct contrast to the gas-phase sidestream spectra, which exhibit significantly higher nicotine

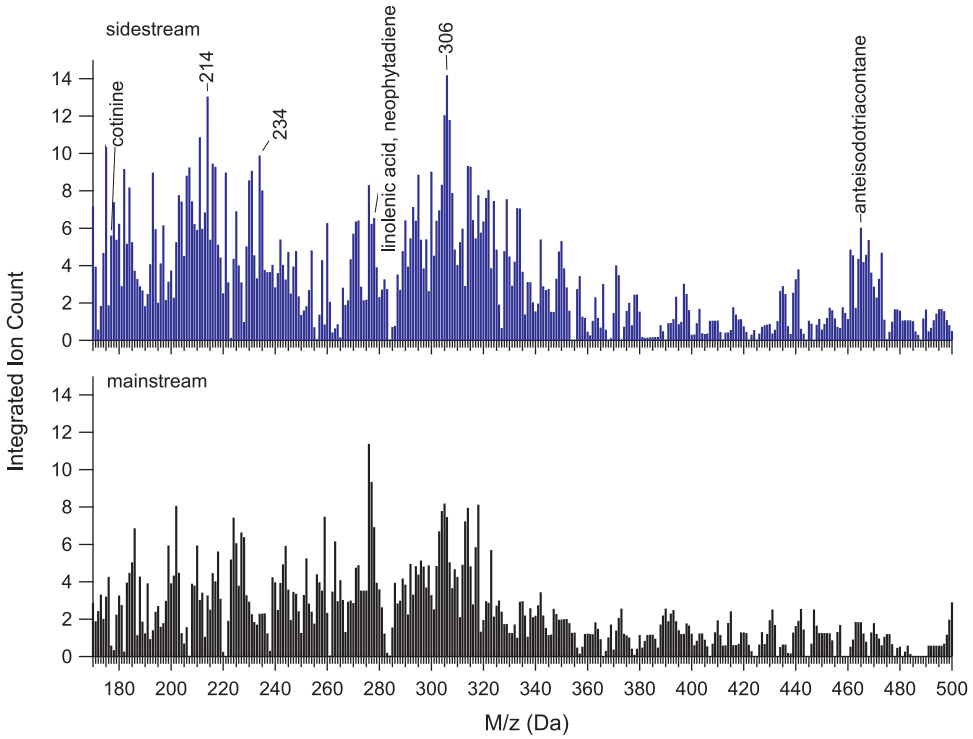

Fig. 7. Comparison of higher molecular weight ions between mainstream and sidestream particle-phase samples from 1R5F cigarette standard.

Table 2
Most prevalent particle-phase compounds as reported by Rogge et al. (1994) and Benner et al. (1989).

Compound	Emission rate (Rogge et al., 1994) (μg/cig)	Collected conc. (Benner et al., 1989) (μmol/g)	M_w (g/mol)
Nicotine	2000	467 ± 144	162.2
Palmitic acid	344.4		256.4
Hydroquinone	283.5		110.1
Stigmasterol	252.2		412.7
Hentriacontane	200.6		436.8
Myosmine	177.9	35 ± 21	146.2
3-hvdroxypyridine	128.6	2.9 ± 1.6	95.1
Tritriacontane	102.3		464.9
β-sitosterol	100.4	2.2 ± 1.8	414.7
Campesterol	92.8	1.53 ± 0.58	400.7
Neophytadiene	81.6		278.5
Anteisodotriacontane	79.1		464.9
Isohentriacontane	78.7		450.8
Heptadecanoic acid	73.0		270.5
Linolenic acid	62.0		278.4
Heptacosane	59.2		380.7
Nonacosane	58.0		408.8
3-pyridinol	57.8		95.0
Cotinine	52.8	20 ± 11	176.2
Nicotyrine	N/A	14 ± 11	158.2
Cholesterol	23.3	1.41 ± 0.33	386.7

content in the 3R4F cigarette.

Fig. 7 displays a comparison of the higher molecular weight ions between the mainstream and sidestream particle-phase spectra for the 1R5F cigarette standard. Quantifying the total mass of these higher molecular weight compounds present in the particle-phase is complicated by a number of factors, including the unknown mass biases associated with transmission through the instrument for larger ion masses, a lack of knowledge of the proton transfer reaction rate constant for these compounds, and an increased number of potential isomers. Therefore, at this point, particle-phase spectra may only potentially be used for identification purposes, in conjunction with a second dimension of measurement (e.g., a simultaneous ion mobility measurement). Table 2 lists those compounds that have been identified by off-line methods as the most prevalent, on a mass basis, in the particle phase. Comparison of Table 2 with Fig. 7 does not demonstrate a large correlation for $m/z > 170$ Da, other than a few selected compounds labeled in the figure. The larger signal for ions between m/z 290 and 320 for both sample streams do not coincide with the most prevalent compounds from Table 2. Nevertheless, CIMS-TOF analysis of larger molecular weight compounds in the particle phase may be used to directly compare two samples, such as the mainstream and sidestream displayed in Fig. 7.

4. Conclusion

The present study demonstrates the potential of CIMS-MS as a relatively comprehensive method for real-time analysis of gas- and particle-phase components of an organic aerosol sample, future work should be done to address some of the limitations of the present study – particularly concerning mass quantification for high-molecular weight particle-phase compounds. Online determination of mass concentration could be accomplished through adequate calibration of the CIMS-MS for each compound of interest.

A benefit of the simultaneous analysis of the gas- and particle-phase in cigarette smoke is the enhanced ability to elucidate the gas/particle partitioning behavior of certain prevalent compounds in cigarette smoke, such as those determined in this study. The concentration of these compounds in the condensed phase may affect the toxicity of smoke particles and how they are absorbed into tissue. For example, it has been determined that multiple organic compounds in ultrafine particles collected from a polluted urban atmosphere work in concert upon inhalation to infiltrate tissue and induce damage to epithelial cells (Li et al., 2003). A related concern about the health effects of cigarette smoke involves the continued outgassing of smoke particles long after they have deposited onto clothing and other fabric. This so-called third-hand smoke refers to sustained high levels of gas-phase nicotine and other semi-volatile compounds, as well as products of indoor chemistry that often involves the oxidation and nucleation of these compounds into breathable ultrafine particles (Burton, 2011).

References

Barsanti, K. C., Luo, W., Isabelle, L. M., Pankow, J. F., & Peyton, D. H. (2007). Tobacco smoke particulate matter chemistry by NMR. *Magnetic Resonance in Chemistry*, *45*(2), 167–170. http://dx.doi.org/10.1002/mrc.1939.

Benner, C. L., Bayona, J. M., Caka, F. M., Tang, H., Lewis, L., Crawford, J., ... Lewis, E. A. (1989). Chemical composition of environmental tobacco smoke. 2. Particulate-phase compounds. *Environmental Science and Technology*, *23*(6), 688–699. http://dx.doi.org/10.1021/es00064a007.

Brunnemann, K. D., Kagan, M. R., Cox, J. E., & Hoffmann, D. (1990). Analysis of 1,3-butadiene and other selected gas-phase components in cigarette mainstream and sidestream by gas chromatography-mass selective detection. *Carcinogenesis*, *11*, 1863–1868. http://dx.doi.org/10.1093/carcin/11.10.1863.

Burton, A. (2011). Does the smoke ever really clear? *Environmental Health Perspectives*, *119*(2), A71–A74.

Chen, B. T., Namenyi, J., Yeh, H. C., Mauderly, J. L., & Cuddihy, R. G. (1990). Physical characterization of cigarette smoke generated from a Walton smoke machine.

Aerosol Science and Technology, *12*, 364–375.
Chen, C., & Pankow, J. F. (2009). Gas/particle partitioning of two acid-bsae active compounds in mainstream tobacco smoke: nicotine and ammonia. *Journal of Agriculture and Food Chemistry*, *57*, 2678–2690.
Eatough, D. J., Benner, C. L., Bayona, J. M., Richards, G., Lamb, J. D., Lee, M. L., ... Hansen, L. D. (1989). Chemical composition of environmental tobacco smoke. 1. Gas-phase acids and bases. *Environmental Science and Technology*, *23*, 679–687.
Eschner, M. S., Selmani, I., Gröger, T. M., & Zimmermann, R. (2011). Online comprehensive two-dimensional characterization of puff-by-puff resolved cigarette smoke by hyphenation of fast gas chromatography to single-photon ionization time-of-flight mass spectrometry: quantification of hazardous volatile organic compounds. *Analytical chemistry*, *83*(17), 6619–6627.
Hanson, D. R., Greenberg, J., Henry, B. E., & Kosciuch, E. (2003). Proton transfer reaction mass spectrometry at high drift tube pressure. *International Journal of Mass Spectrometry*, *223–224*, 507–518.
Hearn, J. D., & Smith, G. D. (2006). Reactions and mass spectra of complex particles using aerosol CIMS. *International Journal of Mass Spectrometry*, *258*, 95–103.
Hertz, R., Streibel, T., Liu, C., McAdam, K., & Zimmermann, R. (2012). Microprobe sampling-photoionization-time-of-flight mass spectrometry for in situ chemical analysis of pyrolysis and combustion gases: Examination of the thermo-chemical processes within a burning cigarette. *Analytica Chimica Acta*, *714*, 104–113.
Hinds, W. C. (1999). *Aerosol Technology* New York: Wiley-Interscience.
Johnstone, R. A. W., & Plimmer, J. R. (1959). The chemical constituents of tobacco and tobacco smoke. *Chemical Reviews*, *59*, 885–936.
Khachatryan, L., Asatryan, R., McFerrin, C., Adounkpe, J., & Dellinger, B. (2010). Radicals from the gas-phase pyrolysis of catechol. 2. Comparison of the pyrolysis of catechol and hydroquinone. *Journal of Physical Chemistry A*, *114*, 10110–10116.
Li, N., Sioutas, C., Cho, A., Schmitz, D., Misra, C., Sempf, J., ... Nel, A. (2003). Ultrafine particle pollutants induce oxidative stress and mitochondrial damage. *Environmental Health Perspectives*, *111*, 455–460.
Mantz, A. W. (2007). Editorial comment. *Spectrochim. Acta. A*, *67*, 1–3.
Mitschke, S., Adam, T., Streibel, T., Baker, R. R., & Zimmermann, R. (2005). Application of time-of-flight mass spectrometry with laser-based photoionization methods for time-resolved on-line analysis of mainstream cigarette smoke. *Analytical Chemistry*, *77*, 2288–2296.
Morrical, B. D., Fergenson, D. P., & Prather, K. A. (1998). Coupling two-step laser desorption/ionization with aerosol time-of-flight mass spectrometry for the analysis of individual organic particles. *Journal of the American Society of Mass Spectrometry*, *9*, 1068–1073.
Northway, M. J., Jayne, J. T., Toohey, D. W., Canagaratna, M. R., Trimborn, A., Akiyama, K. I., ... Worsnop, D. R. (2007). Demonstration of a VUV lamp photoionization source for improved organic speciation in an aerosol mass spectrometer. *Aerosol Science and Technology*, *41*, 828–839.
Oktem, B., Tolocka, M. P., & Johnston, M. V. (2004). On-line analysis of organic components in fine and ultrafine particles by photoionization aerosol mass spectrometry. *Analytical Chemistry*, *76*, 253–261.
Pankow, J. F. (2001). A consideration of the role of gas/particle partitioning in the deposition of nicotine and other tobacco smoke compounds in the respiratory tact. *Chemical Research in Toxicology*, *14*, 1465–1481.
Philippe, R. J., & Hobbs, M. E. (1956). Some components of the gas phase of cigarette smoke. *Analytical Chemistry*, *28*, 2002–2006.
Pieraccini, G., Furlanetto, S., Orlandini, S., Bartolucci, G., Giannini, I., Pinzauti, S., & Moneti, G. (2008). Identification and determination of mainstream and sidestream smoke components in different brands and types of cigarettes by means of solid-phase microextraction–gas chromatography–mass spectrometry. *Journal of Chromatography A*, *1180*(1–2), 138–150.
Report on Carcinogens (2011). U.S. Department of Health and Human Services. 〈https://www.ncbi.nlm.nih.gov/pubmed/21822324〉.
Rogge, W. F., Hildemann, L. M., Mazurek, M. A., Cass, G. R., & Simoneit, B. R. (1994). Sources of fine organic aerosol. 6. Cigarette smoke in the urban atmosphere. *Environmental Science and Technology*, *28*, 1375–1388.
Spanel, P., & Smith, D. (1998). Selected ion flow tube studies of the reactions of H_3O^+, NO^+, and O_2^+ with several aromatic and aliphatic hydrocarbons. *International Journal of Mass Spectrometry*, *181*, 1–10.
Spears, A. W. (1963). Quantitative determination of phenol in cigarette smoke. *Analytical Chemistry*, *35*, 320–322.
Tang, X., Zheng, Z., Jung, H. S., & Asa-Awuku, A. (2012). The effects of mainstream and sidestream environmental tobacco smoke composition for enhanced condensational droplet growth by water vapor. *Aerosol Science and Technology*, *46*(2012), 760–766.
Tanimoto, H., Aoki, N., Inomata, S., Hirokawa, J., & Sadanaga, Y. (2007). Development of a PTR-TOFMS instrument for the real-time measurements of volatile organic compounds in air. *International Journal of Mass Spectrometry*, *263*, 1–11.
Zhao, J., & Zhang, R. (2004). Proton transfer reaction rate constants between hydronium ion and volatile organic compounds. *Atmospheric Environment*, *38*, 2177–2185.